利用卷對卷製造技術轉移大面積電化學剝離石墨烯於軟性基材表面並對於其光電熱特性之研究

胡龍豪

南臺科技大學機械工程系

lunghhu@stust.edu.tw

摘要

由於石墨烯良好的導熱性、透光性及導電性。因此，其為目前最有機會取代傳統金屬氧化物，作為軟性電子元件及顯示器的材料之一。而石墨烯平面熱傳導係數 (2000~5300 $Wm^{-1}K^{-1}$) 以及內部載子移動率 (2×10^5 $cm^2V^{-1}s^{-1}$) 都相當的高。而這些光電熱特性則因石墨烯生產時的層數有著極大的影響。然而，目前業界仍然缺少了，可大量生產高品質且低成本石墨烯的技術。而電化學剝離石墨烯生產技術，則提供了一個由便宜的石墨原料生產大量高品質石墨烯的技術。由此技術生產出來的石墨烯大多為雙層或多層石墨烯，而它們剝離下來的尺寸可達到數十微米等級。由拉曼光譜分析可知，電化學剝離石墨烯的品質優於傳統之氧化還原石墨烯。利用轉移電化學剝離石墨烯至可饒透明基材上可製造出可饒透明導電膜。而透過這樣卷對卷的生產方式，則可以很容易地製造出大面積的可饒透明石墨烯導電膜。而其片電阻及熱電特性因數則由其層數所影響，而石墨烯的層數(厚度)則由其穿透度來定義。由紫外光-可見光光譜儀量測其穿透度可達 85 %。

關鍵詞：電化學剝離石墨烯、片電阻、卷對卷製造技術、熱電特性因數

Thermal, Electrical and Optical Properties of Electrochemically Exfoliated Graphene on Flexible Substrate via Roll-to-Roll Fabrication

Lung-Hao Hu

Department of Mechanical Engineering, Southern Taiwan University of Science and Technology

Abstract

Graphene is a promising candidate for replacing some metal oxide-based materials. Due to its high conductivity and flexability, it can fabricated into transparent and supple conducting electrodes used in displays and electronic devices. Its in-plane thermal conductivity (2000~5300 $Wm^{-1}K^{-1}$) and intrinsic carrier mobility (2×10^5 $cm^2V^{-1}s^{-1}$) are extremely high, depending on the size of graphene flake and number of graphene layers, as well as its quality. However, currently there is still no good method to provide high-quality, low-cost graphene in large quantities. Electrochemically exfoliated graphene enables the fabrication of massive graphene sheets in an ink form using artificial graphite as the starting material. This product is mainly composed of bi-layer and multi-layered graphene. Its lateral size can reach over ten μm, and the quality as measured by Raman spectroscopy has been shown to be higher than that of the reduced graphene oxide. The transparent and flexible conducting films made of the electrochemically exfoliated graphene can be simply transferred from the graphene ink onto any flexible and transparent substrate, such as polyethylene terephthalate, which is easy to scale up for large-area deposition via roll-to-roll fabrication. The sheet resistance and thermoelectric figures of merit, ZT of the

Received: May 31, 2017; first revised: Aug. 20, 2017; accepted: Oct. 2017.
Corresponding author: L.-H. Hu, Department of Mechanical Engineering, Southern Taiwan University of Science and Technology, Tainan, Taiwan.

electrochemically exfoliated graphene, have been measured as a function of its thickness as specified by its transmittance (85%), determined by a UV-Vis spectrometer, and the thermal conductivity can be determined through its thermoelectric properties.

Keywords: Electrochemically Exfoliated Graphene, Sheet Resistance, Roll-to-roll Fabrication, Thermoelectric Figures of Merit

I. Introduction

The recent research is focusing on the intense interest of graphene applications due to its extremely high aspect ratio and unique physical properties (A.K. Geim and K.S. Novoselov., 2007), such as superior electrical conductivity (10^6 $\Omega^{-1}cm^{-1}$), high carrier mobility (2×10^5 cm^2/Vs; silicon: 1,400 cm^2/Vs) measured by Zhang et al. (2005) and Chen et al. (2008), almost transparent in visible light (97.7 %) detected by Li et al.(2009) , excellent mechanical strength (Young's modulus > 1 TPa) measured by Lee et al. (2008), good bendability and its extremely high thermal conductivity and transparency [1]. The thermal conductivity of graphene can reach the range of 2000–5300 $Wm^{-1}K^{-1}$ near room temperature depending on the lateral dimensions of the graphene flakes [2-3]. Graphene paper has also been introduced to apply to thermal management for electronic devices (Gee et al., 2014)[4]. Due to these promising properties mentioned above, graphene plays an important role to be a good candidate as transparent conducting electrodes for the applications in touch screens, flexible displays, printable electronics, and solar cells. Indium tin oxide (ITO) or aluminum-doped zinc oxide (AZO) commonly and commercially used in portable electronic devices has the drawbacks of brittle nature and growing cost, thus not being compatible with the requirements of next-generation flexible devices. Graphene would be highly promising for a replacement of the oxide-based materials. Su et al. (2011) has demonstrated a one-step process to synthesize graphene thin sheets by electrochemical exfoliation of graphite [5]. The sample's lateral size can reach tens μm, and their quality determined by Raman spectroscopy is much better than reduced GO. The high-cost graphite flake is replaced with the low-cost artificial graphite to prepare the samples. The results indicate that massive graphene sheets can be successfully obtained by exfoliating artificial graphite using the same electrochemical method. The quality, morphology, and size of the products are investigated and discussed. Here we report a novel transferring technique using the electrochemically exfoliated graphene (ECG) to make the graphene film on the flexible substrate, polyethylene terephthalate (PET) and measure its thermoelectric and optical properties. Here the thermoelectric properties of the electrochemically exfoliated graphene (ECG) can be evaluated by the thermoelectric figure of merit *ZT* formulated as $ZT=(S^2\sigma/k)T$, where *S, σ, k and T* are the thermaopower (or Seebeck coefficient), electrical conductivity, thermal conductivity and temperature in Kevin, respectively, and the optical property is evaluated by transmittance determined by UV-Vis spectrometer[2-3].

II. Experimental

1. Electrochemically exfoliated graphene

Our samples were synthesized by electrochemical exfoliation method as shown in Fig.1. The set-up was with a piece of artificial graphite as the working electrode and a platinum wire served the purpose of a reference electrode. The electrolyte was a mixture of H_2SO_4 and KOH (composition: 2.4 g of H_2SO_4 and 11 ml 30% KOH in 100 ml DI water). A DC bias was applied to the working electrode (±20 V) for the electrochemical reaction. The following steps show the voltage program: (1) +2.5 V for 60 sec; (2) +20 V for 5 sec; (3) –20 V for 5 sec.

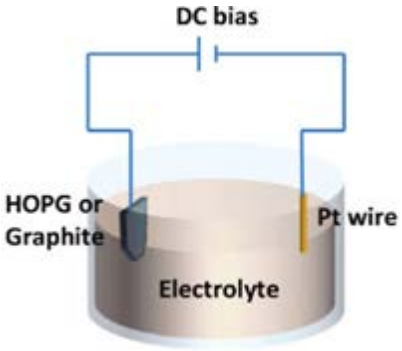

Fig.1 The scheme of the electrochemically exfoliated process[1]

steps. (2) and (3) are repeated alternatively until the amount of the product reaches our requirement. The products were then vacuum-filtrated by a filter membrane (pore size ≈ 0.2 μm) and rinsed with DI water and ethanol to remove the residual electrolyte. The purified flake was partially dried at 100 ºC for 10 min on hot plate. The sample has to be maintained under a partially dried status; otherwise, the graphene layers will tightly stack to cause the difficulty to disperse in further process. To obtain well-dispersed samples, one-minute sonication was carried out the products with 0.1wt% of graphene in *N*,*N*-dimethylformamide (DMF). Finally, the unreacted starting materials are removed by filtering the dispersion. The thickness of ECG film on PET depends on the number of transferring times from the graphene ink. The morphologies of the samples were characterized by optical microscope (OM), atomic force microscope (AFM, Veeco Dimension-Icon system), and scanning electron microscope (SEM, JEOL JSM-6500F). The quality of graphene sheets was identified using Raman spectroscopy (NT-MDT NTEGRA, wavelength: 473 nm)[5].

2. Transferring of ECG on PET via roll-to-roll fabrication

The graphene ink synthesized by electrochemical process was drop-wised onto a water bath. Owing to its hydrophobic property, the graphene flakes were self-assembling on water surface. A large and long PET roll-sheet (180μm thick) was immersed into the water bath connected to one cylindrical roller with a tilt angle to contact the self-assembled graphene region and the other end of the PET roll-sheet is connected to the other cylindrical roller. Then the PET sheet was slowly pulled out by rotating the roller from the water bath with the graphene flakes attached. The scheme of transferring ECG is illustrated in Fig.2.

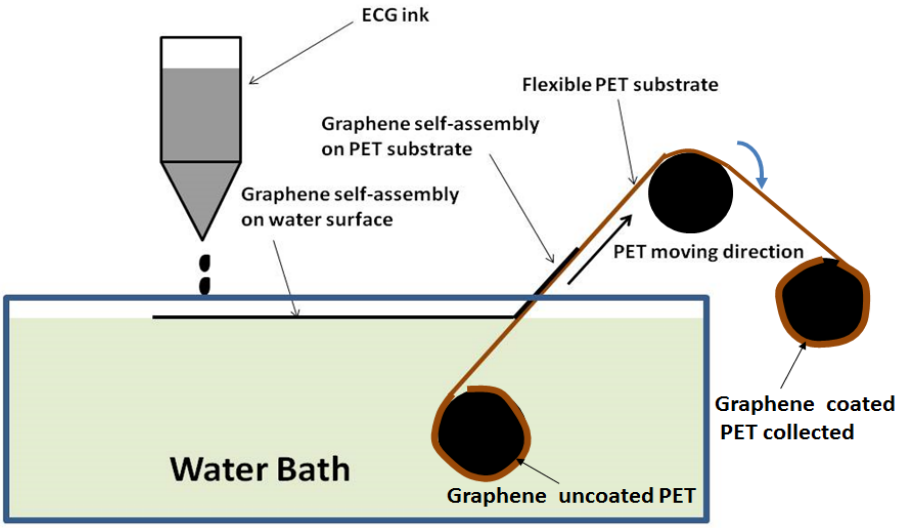

Fig.2 The scheme of transferring technique of ECG on PET via roll-to-roll fabrication

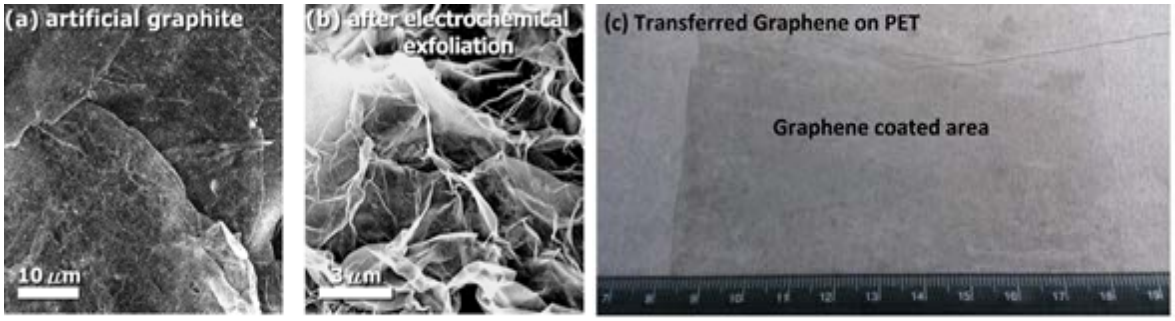

(a) the starting material, artificial graphite (b) the artificial graphite electrochemically exfoliated
(c) the Photograph of the large scale transferring of ECG on PET

Fig.3 The SEM image

Due to the surface roughness and adhesion of PET, the bonding is very strong between the PET surface and ECG. The thickness of ECG on PET can be controlled by the number of transferring times; however, the more transferring times applied, the lower transmittance achieved. Fig.3 displays the scanning electron microscope (SEM) images of the artificial graphite (starting material, Fig.3a), ECG (Fig.3b) and the transferred ECG on PET (Fig.3c), respectively.

3. Thermoelectric method for in-plane thermal conductivity

Hall Effect measurement based on Van der Pauw method was carried out for clarifying the electrical properties of ECG on PET to obtain its electrical conductivity incorporated with the thermal electric figure-of-merit (FOM), ZT. After the seebeck coefficient is measured, the in-plane thermal conductivity can be obtained. The area of each ECG on PET measured is 1.5 cm by 1.5 cm. The thickness of ECG on PET was controlled by the transferring times, in this study; we transferred ECG on PET with one, two, three, and five times for the identification of different thickness. The pure PET and different thickness of ECG transferred on PET are shown in Fig.4. The transmittance of the samples was determined by UV-Vis spectrometer at 550 nm wavelength to be a function of the thickness.

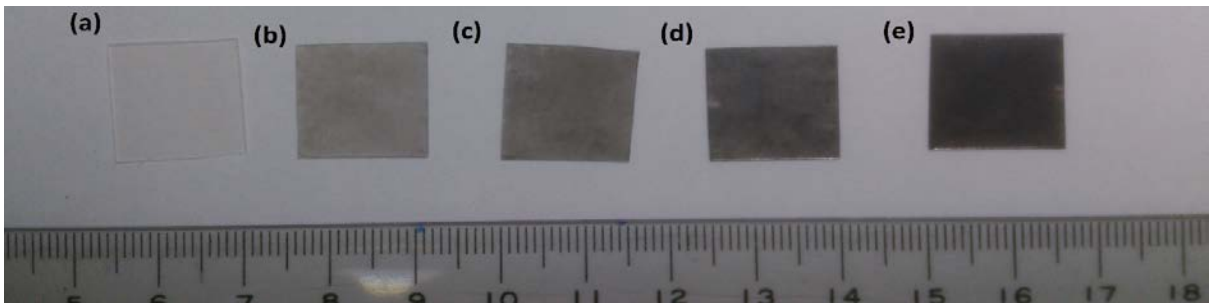

(a) Pure PET (b) one time (b) twice (c) three times (d) five times transfer

Fig.4 the photograph of different thickness of ECG transferred on PET

III. Results and Discussion

1. Electrochemically Exfoliated Graphene

The working electrode for the electrochemical exfoliation process is artificial graphite, reacting at the programmed voltage (±20 V) in a mixed electrolyte solution (H_2SO_4 + KOH). The intercalation into graphite layers relies on the use of sulfate ions (SO_4^{2-}) by applying a positive bias to the working electrode. The addition

of hydroxyl ions (OH^-) is to partially neutralize the electrolyte for avoiding oxidation of the products during the reaction. The optimization of applied voltage is needed depending on the kind of starting materials. The exfoliation process cannot occur, if the bias is too low, whereas the electrode could be destroyed under a very high bias because of strong intercalation behavior. After reaction, the residual electrolyte was removed from the products by vacuum filtration and rinsing with DI water and ethanol for several times until the pH is close to neutral. The uniform stable dispersion of the graphene ink is achieved by sonicating the purified samples in N, N-dimethylformamide (DMF) for 1 min as shown in Fig. 5(a). The products deposited on 300 nm SiO_2/Si substrate by dip-coating is shown in Fig. 5(b). The lateral size of these sheets is over ten μm. The confocal Raman spectra (excited by 473 nm laser; power: 0.5 mW; spot size: ≈ 0.5 μm) for starting material and exfoliated graphene sheets is shown in Fig. 5(c), respectively. AFM was used to measure the layer number of the samples transferred on silicon substrate as shown in Fig. 5(d). The thickness of ECG each transfer measured from the edge is around 2.2 nm, also corresponding to the characteristic of bi-layer graphene (Su et al., 2011). The strong G-band (at 1578.4 cm^{-1}) and tiny D-band (near 1360 cm^{-1}) from the artificial graphite indicate a feature of well-crystallized bulk graphite [6-10]. After the starting material exfoliated, the D-band greatly increases and a shift of G-band (at 1591.8 cm^{-1}) appears. It is known that the I_{2D}/I_G ratio of bi-layer graphene is lower than that of monolayer one [6-11]. The I_D/I_G ratio is 1.21, suggesting that graphene surface is partially oxidized because of sulfuric acid intercalation. The appearance of disorder-induced D-band can be attributed to the formation of nanodomains in graphene lattice during exfoliation. Note that the 2D-band (at ≈ 2700 cm^{-1}) is composed of four components ($2D_{1B}$, $2D_{1A}$, $2D_{2A}$, $2D_{2B}$) and is an asymmetric peak, except the case of monolayer graphene. In the inset of Fig. 5(c), the sample shows an asymmetric 2D-band, but the intensity of the higher frequency 2D2 peaks is not dominant, suggesting that our product is mainly bi-layer graphene. Additionally, the larger I_{2D}/I_G ratio (the integrated peak ratio between 2D- and G-bands) represents higher degree of crystallization for sp^2 C=C bonds in graphene structure (Krauss., 2009). Although our sample is as-prepared and without any reduction treatment, its I_{2D}/I_G ratio (0.36) is still higher than that of GO, even which is reduced by hydrazine and 800 °C-annealing (Su et al., 2009)[12-13].

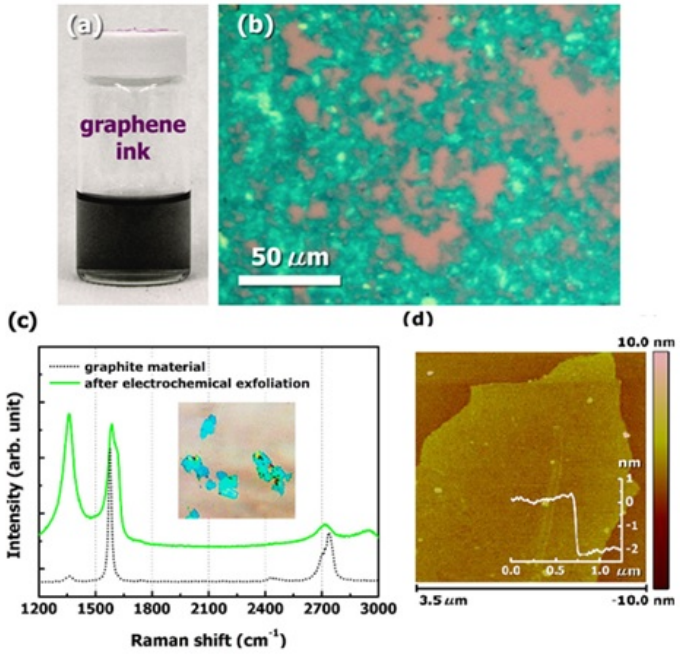

(a) picture of electrochemically exfoliated graphene dispersed in DMF (b) the OM image of graphene thin sheets (c) Raman spectra of starting material and the product after reaction (d) AFM scan of single ECG transferred on SiO_2/Si

Fig.5 Optical microscope image, Raman spectra and AFM image

2. Morphologies of ECG

The morphologies of the starting material and exfoliated graphene were observed under SEM as shown in Fig. 3a and b, respectively; the surface of artificial graphite shown in Fig. 3(a) is smooth and reveals a laminar microstructure. On the contrary, in Fig. 3(b) the starting material electrochemically exfoliated is substantially comprised of wrinkled and folded thin sheets.

3. Electrical and optical Properties of ECG on PET

The sheet resistance was measured by the Hall Effect measurement based on Van der Pauw method with the different thickness of transferred ECG on PET cut into pieces with each area of 1.5 cm by 1.5 cm as shown in Fig.4 [14-16]. The sheet resistance is formulated as $R=\rho(L/A)$, where R is the sheet resistance measured by the Hall effect measurement, ρ is the resistivity, L and A are the geometric factors of thickness and area of ECG on PET, respectively. While decreasing the number of times for ECG transferring, the sheet resistance is increased by one order for each transfer time added as shown in Fig.6 (a) and (b). The Fig 6 (b). shows the sheet resistances of ECG with the thickness, 4.4 nm, 6.6 nm and 11nm.

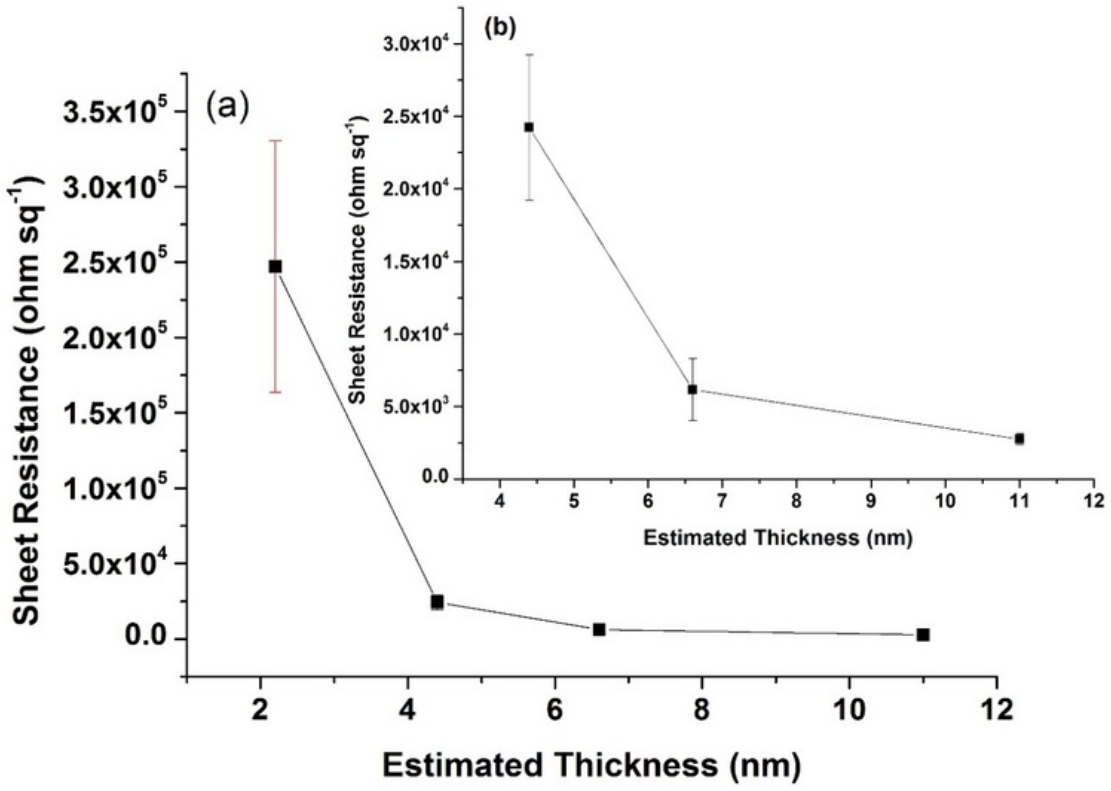

(a) sheet resistances with different estimated thickness of ECG on PET
(b) sheet resistances of ECG with the estimated thickness of 4.4 nm, 6.6 nm and 11 nm on PET

Fig.6 Sheet resistances

The thickness of ECG on PET is difficult to be preciously measured due to the overlapped and uncovered regions of ECG during transferring. The thickness can be estimated by AFM scan for each transfer as shown in Fig.5 (d). Owing to the difficulty to evaluate the real thickness of each ECG transfer, UV-Vis spectrometer was used to define the thickness of ECG [14-16]. The transmittance is linearly inverse proportional to the thickness of ECG transferred as shown in Fig.7.

One time transfer of ECG can achieve the transmittance around 84%. Because the estimated thickness is not a precisely accurate value to define the number of layers of ECG transferred, a well-defined index is needed to evaluate the optical property corresponding to the layers; therefore, sheet resistance and transmittance are plotted to well-define the optical property with respect to the number of layers of ECG transferred as shown in Fig.8 that displays an almost matched plot compared to Fig.6. This indicates that to use the number of transferring times to evaluate the thickness of ECG on PET gives high accuracy.

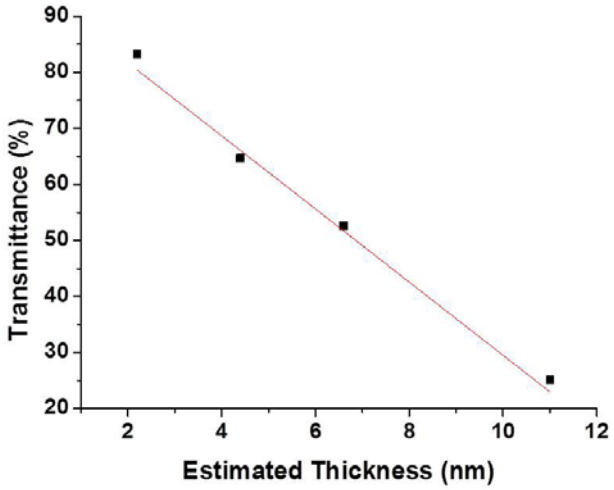

Fig.7 Transmittance with different thickness of ECG o PET

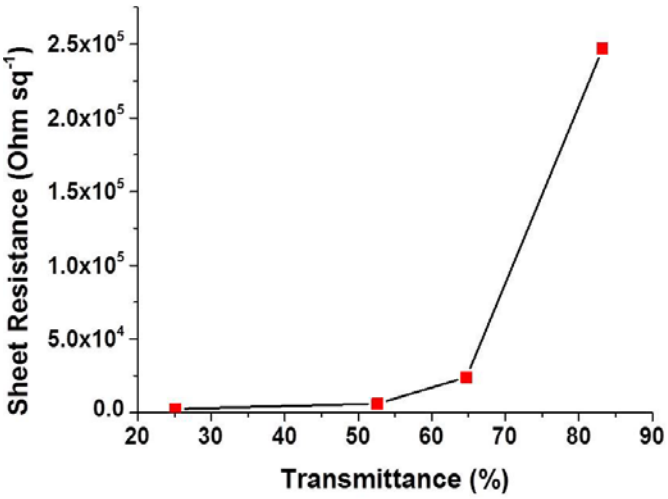

Fig.8 Transmittance with respect to the sheet resistance

4. Thermal and electrical properties of ECG on PET

The thermoelectric experiment has been introduced to measure the thermal property of graphene paper (Gee et al., 2014)[4]. We used the same experimental set-up to measure the thin ECG on PET. The thermoelectric properties of the electrochemically exfoliated graphene (ECG) can be evaluated by the thermoelectric figure of merit ZT formulated as $ZT=(S^2\sigma/k)T$, where S, σ, k and T are the thermaopower (or Seebeck coefficient), electrical conductivity, in-plane thermal conductivity and temperature in Kevin, respectively, and the electrical conductivity can be obtained from the sheet resistance. An electrical potential, $V_{out}=V_1-V_2$, produced by a temperature difference, which is created by pumping an electrical current into thermal electric material [2,11,14]. Fig.9

displays the seebeck coefficients of different ECG transferring times that the result shows the thermopower (The slope in Fig.9) remains the same value~30 (V/ ºC) ; it is indicated to the independence of the thickness of ECG transferred. The reason could be that the thickness is too thin, compared to the PET substrate to precisely evaluate the seebeck coefficient. Also the ZT value is too small to be measured. The thermoelectric effect cannot be obviously observed in this case. Table 1 is the summary of the thermoelectric property with different thickness of ECG on PET.

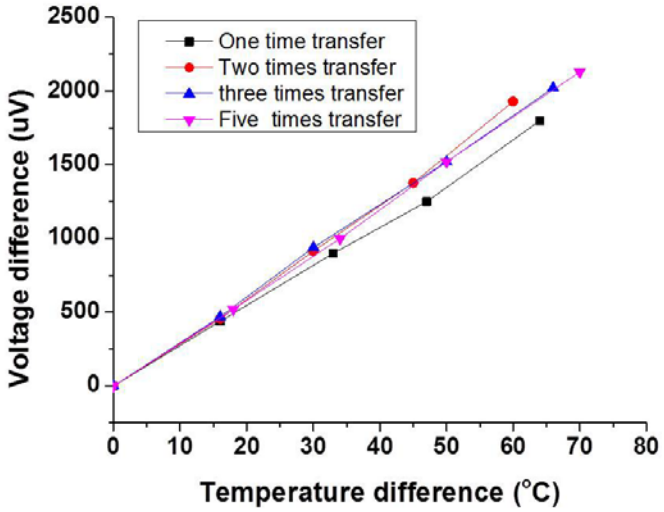

Fig.9 Thermopower (Seebeck coefficient) with different thickness of ECG on PET

Table 1. The thermoelectric property of ECG on PET

Transferring times	1	2	3	5
Seedback (S)	30.4	30.75	29.7	30.4
ZT	0	0	0.02	0.02
σ	$8.91X10^{-11}$	$1.82X10^{-9}$	$1.07X10^{-8}$	$4.01X10^{-8}$
T	293K	293K	293K	293K

IV. Conclusions

Here, we report a low-cost roll-to-roll transferring technique to transfer the electrochemically exfoliated graphene in large-scale onto the flexible substrate. The transmittance of the large-scale conducting and flexible electrode can reach around 84%~90% for single time ECG transfer. The thermoelectric effect cannot be obviously observed in this case owing to the thickness of ECG on PET is too thin compared to the PET substrate and the thermo-power is independent of the thickness of ECG. The flexible substrate with large-scale graphene coating would be a potential application for the next generation touch screen and panel.

References

[1] J. H. Chen, C. Jang, S. D. Xiao, M. Ishigami, and M. S. Fuhrer. (2008). Intrinsic and extrinsic performance limits of graphene devices on SiO_2. *Nature Nanotechnology, 3*, 206-209.

[2] J. G. Checkelsky, and N. P. Ong. (2009). The thermopower and nerst effect in graphene in a magnetic field. *Physical Review B, 80*, 081413(R)

[3] A. C. Ferrari, J. C. Meyer, V. Scardaci, C. Casiraghi, M. Lazzeri, F. Mauri, S. Piscanec, D. Jiang, K. S. Novoselov, S. Roth, and A. K. Geim. (2006). Raman spectrum of graphene and graphene layers, *Physical Review Letters, 97*(18), 187401.

[4] A. K. Geim, and K. S. Novoselov. (2007). The rise of graphene. *Nature Materials, 6*(3), 183-191.

[5] C. M. Gee, C. C. Tseng, F. Y. Wu, C. T. Lin, H. P. Chang, L. J. Li, J. C. Chen, and L. H. Hu. (2014). Few layer graphene paper from electrochemical process for heat conduction. *Materials Research Innovations, 18*(3), 208-213.

[6] C. Y. Su, A. Y. Lu, Y. P. Xu, F. R. Chen, A. N. Khlobystov, and L. J. Li. (2011) High-quality thin graphene films from fast electrochemical exfoliation. *ACS Nano, 5*(3), 2332–2339.

[7] A. Gupta, G. Chen, P. Joshi, S. Tadigadapa, and P. C. Eklund. (2006). Raman scattering from high-frequency phonons in supported n-graphene layer films. *Nano Letters, 6*(12), 2667-2673.

[8] B. Krauss, T. Lohmann, D. H. Chae, M. Haluska, K. von Klitzing, and J. H. Smet. (2009). Laser-induced disassembly of a graphene single crystal into a nanocrystalline network. *Physical Review B, 79*(16), 165428.

[9] X. S. Li, Y. W. Zhu, W. W. Cai, M. Borysiak, B. Y. Han, D. Chen, R. D. Piner, L. Colombo, and R. S. Ruoff. (2009). Transfer of large-area graphene films for high-performance transparent conductive electrodes. *Nano Letters, 9*(12), 4359-4363.

[10] C. Lee, X. D. Wei, J. Kysar, and W. J. Hone. (2008). Measurement of the elastic properties and intrinsic strength of monolayer graphene. *Science, 321*(5887), 385-388.

[11] Z. H. Ni, H. M. Wang, J. Kasim, H. Fan, M. T. Yu, Y. H. Wu, Y. P. Feng, and Z. X. Shen. (2007). Graphene thickness determination using reflection and contrast spectroscopy. *Nano Letters, 7*(9), 2758-2763.

[12] X. X. Ni, G. C. Liang, J. S. Wang, and B. W. Li.(2009). Disorder Enhanceds Thermoelectrics Figure of merit in Armchair Graphene Nanoribbons. *Applied Physical Letters, 95*,192114.

[13] C. Y. Su, Y. P. Xu, W. J. Zhang, C. H. Tasi, J. W. Zhao, X. H. Tang, and L. J. Li. (2009). Electrical and Spectroscopic Characterizations of Ultra-Large Reduced Graphene Oxide Monolayers. *Chemistry of Materials, 21*(23), 5674-5680.

[14] J. K. Wassei, and R. B. Kaner. (2010). Graphene, a promising transparent conductor. *Materials Today 13*(3), 52-59.

[15] P. Wei, W. Bao, Y. Pu, C. N. Lau, and J. Shi. (2009). Anomalous thermoeletric transport of dirac particles in graphene. *Physical Review Letters, 102*(16),166808

[16] K. Yan, H. L. Peng, Y. Zhou, H. Li, and Z. F. Liu. (2011). Formation of bilayer bernal graphene: layer-by-layer epitaxy via chemical vapor deposition. *Nano Letters, 11*(3), 1106-1110.

[17] Y. B. Zhang, Y. W. Tan, H. L. Stormer, and P. Kim. (2005). Experimental observation of the quantum Hall effect and Berry's phase in graphene. *Nature, 438*, 201-204.